arXiv:1403.3484v1 [cond-mat.quant-gas] 14 Mar 2014

First and second sound in a two-dimensional dilute Bose gas across the Berezinskii-Kosterlitz-Thouless transition

Xia-Ji Liu[1] and Hui Hu[1]
[1] *Centre for Quantum and Optical Science, Swinburne University of Technology, Melbourne 3122, Australia*
(Dated: March 17, 2014)

We theoretically investigate first and second sound of a two-dimensional (2D) atomic Bose gas in harmonic traps by solving Landau's two-fluid hydrodynamic equations. For an isotropic trap, we find that first and second sound modes become degenerate at certain temperatures and exhibit typical avoided crossings in mode frequencies. At these temperatures, second sound has significant density fluctuation due to its hybridization with first sound and has a divergent mode frequency towards the Berezinskii-Kosterlitz-Thouless (BKT) transition. For a highly anisotropic trap, we derive the simplified one-dimensional hydrodynamic equations and discuss the sound-wave propagation along the weakly confined direction. Due to the universal jump of the superfluid density inherent to the BKT transition, we show that the first sound velocity exhibits a kink across the transition. Our predictions can be readily examined in current experimental setups for 2D dilute Bose gases.

PACS numbers: 67.85.De, 03.75.Kk, 05.30.Jp

Low-energy excitations of a quantum liquid in its superfluid state - in which inter-particle collisions are sufficiently frequent to ensure local thermodynamic equilibrium - can be well described by Landau's two-fluid hydrodynamic theory [1, 2]. It is now widely known that there are two types of excitations, namely first and second sound, which describe respectively the coupled in-phase (density) and out-of-phase (temperature) oscillations of the superfluid and normal fluid components [3]. Historically, Landau's two-fluid hydrodynamic theory was invented to understand the quantum liquid of superfluid helium [2]. The study of first and second sound in such a system has greatly enriched our knowledge of the fascinating but challenging many-body physics. For any new kind quantum fluids, it is therefore natural to anticipate that first and second sound may also provide a powerful tool to characterize their underlying physics.

In this context, the case of a two-dimensional (2D) dilute Bose gas confined in harmonic trapping potentials, which has recently been realized in ultracold atomic laboratory [4–7], is of particular interest. At nonzero temperatures, the condensation of bosonic atoms is precluded by the Hohenberg-Mermin-Wagener theorem [8, 9]. The superfluid phase transition in such a system is of the Berezinskii-Kosterlitz-Thouless (BKT) type [10, 11], whose nature is remarkably different from the conventional second-order phase transition in three dimensions (3D). The BKT transition is associated with the emergence of a topological order, as a result of the pairing of vortices and anti-vortices. Therefore, across the BKT transition from below, the superfluid density of the system jumps to zero from a universal value $4/\lambda_{dB}^2$, where $\lambda_{dB} \equiv \sqrt{2\pi\hbar^2/(mk_BT)}$ is the thermal de Broglie wavelength at the temperature T. In the absence of harmonic traps, this leads to discontinuities in the first and second sound velocities at the BKT transition [12], as illustrated in Fig. 1.

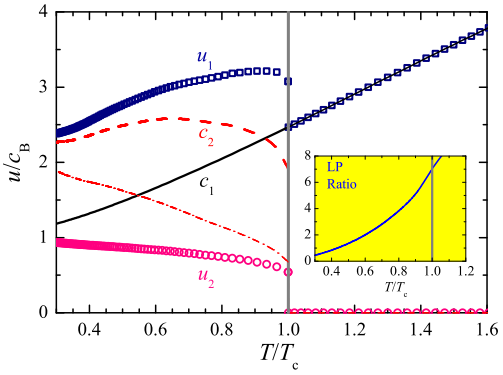

Figure 1: (Color online) First (squares) and second sound velocities (circles) of a uniform 2D Bose gas across the BKT transition temperature T_c, in unit of the Bogoliubov sound velocity c_B. The dimensionless coupling constant $g = 0.05$. For comparison, the decoupled first and second sound velocities are shown by the solid and dashed lines, respectively. The dot-dashed line is the velocity of second sound with the leading-order correction due to its coupling to first sound. The inset shows the Landau-Placzek parameter, which characterizes the coupling between first and second sound.

In this work, we discuss the behavior of first and second sound of a harmonically *trapped* 2D Bose gas. Our investigation is motivated by the recent sound mode measurements in a trapped 3D unitary Fermi gas [13–16], which provide valuable information on its equation of state and superfluid density. In particular, in a milestone experiment performed by the Innsbruck team [16], first and second sound waves were excited in the highly elongated unitary Fermi gas, and their propagations along the weakly confined axis were measured. These measurements are straightforward to implement in a trapped 2D

Bose or Fermi gas, and would greatly promote the current experimental [4–7] and theoretical research [17–19] on the intriguing BKT physics in ultracold atoms and solid-state systems.

Our main results are briefly summarized as follows. In sharp contrast to the superfluid helium and unitary Fermi gas, we find that the coupling between density and temperature oscillations in a 2D Bose gas are very strong, as characterized by a large Landau-Placzek (LP) parameter (see the inset of Fig. 1), thereby making the observation of second sound much easier. The universal jump of superfluid density at the BKT transition leads to non-trivial consequences in the sound mode frequencies and velocities. In an isotropic harmonic trap, we show that the mode frequency of second sounds diverges as $(T-T_c)^{-1/2}$ approaching the BKT critical temperature T_c. While in a highly anisotropic trap, the velocity of the first sound wave propagation in the weakly confined direction exhibits an apparent kink right at the transition. The experimental confirmation of these predictions would provide a complete proof of the BKT physics.

We start by considering an interacting atomic Bose gas trapped in a 2D harmonic potential, $V_T(\mathbf{r}) = m(\omega_x^2 x^2 + \omega_y^2 y^2)/2$, with atomic mass m and trapping frequencies ω_x and ω_y. The motion in the third direction is assumed to be frozen by an additional, tight harmonic confinement, as realized in current experiments [4–7]. First and second sound of the system are described by Landau's two-fluid hydrodynamic equations which involve only local thermodynamic variables and superfluid density. As discussed in the previous works [20–22], using Hamilton's variational principle [23], first and second sound modes of these equations with frequency ω can be obtained by minimizing a variational action, which, in terms of displacement fields $\mathbf{u}_s(\mathbf{r})$ and $\mathbf{u}_n(\mathbf{r})$ for superfluid and normal fluid components, takes the following form [20],

$$S = \frac{1}{2}\int d\mathbf{r}\left[m\omega^2\left(n_s\mathbf{u}_s^2+n_n\mathbf{u}_n^2\right)-\left(\frac{\partial\mu}{\partial n}\right)_s(\delta n)^2 -2\left(\frac{\partial T}{\partial n}\right)_s\delta n\delta s-\left(\frac{\partial T}{\partial s}\right)_n(\delta s)^2\right]. \quad (1)$$

Here, $n(\mathbf{r})$ and $s(\mathbf{r})$ are respectively the local number density and entropy density, $n_s(\mathbf{r})$ and $n_n(\mathbf{r}) = n(\mathbf{r}) - n_s(\mathbf{r})$ are the superfluid and normal-fluid densities at equilibrium, $\delta n(\mathbf{r}) \equiv -\nabla\cdot(n_s\mathbf{u}_s + n_n\mathbf{u}_n)$ is the density fluctuation, and $\delta s(\mathbf{r}) \equiv -\nabla\cdot(s\mathbf{u}_n)$ is the entropy fluctuation. The effect of the harmonic trapping potential $V_T(\mathbf{r})$ enters the action Eq. (1) through the coordinate dependence of the equilibrium thermodynamic variables $(\partial\mu/\partial n)_s$, $(\partial T/\partial n)_s$ and $(\partial T/\partial s)_n$.

For a 2D interacting Bose gas, due to the scale invariance of the interatomic interaction [24], all the thermodynamic inputs can be written in terms of dimensionless universal functions that depend only on the ratio $z(\mathbf{r}) = \mu(\mathbf{r})/k_BT$ and the dimensionless coupling constant $g = \sqrt{8\pi}a_s/l_z$ [17], where $\mu(\mathbf{r}) = \mu - V_T(\mathbf{r})$ is the local chemical potential within local density approximation, a_s is the 3D scattering length, and l_z is the oscillator length in the tight confinement direction. In particular, the local pressure, number density and superfluid density are given by [12], $P(\mathbf{r}) = k_BT\lambda_{dB}^{-2}f_p[g, z(\mathbf{r})]$, $n(\mathbf{r}) = \lambda_{dB}^{-2}f_n[g, z(\mathbf{r})]$ and $n_s(\mathbf{r}) = \lambda_{dB}^{-2}f_s[g, z(\mathbf{r})]$, respectively. These universal functions have been calculated theoretically [17–19] and partly measured experimentally [4, 5], to certain accuracy. Throughout this work, we will use the results determined by Monte Carlo simulations for small interaction parameter g [17, 18].

In superfluid helium [3] and unitary Fermi gas [22], the solutions of Landau's hydrodynamic equations can be well understood as density and temperature waves, which are the pure in-phase mode with $\mathbf{u}_s = \mathbf{u}_n$ and the pure out-of-phase mode with $n_s\mathbf{u}_s + n_n\mathbf{u}_n = 0$, known as first and second sound, respectively [2, 3]. Following this classification, we may rewrite the action Eq. (1) in terms of two new displacement fields $\mathbf{u}_a = (n_s\mathbf{u}_s + n_n\mathbf{u}_n)/n$ and $\mathbf{u}_e = \mathbf{u}_s - \mathbf{u}_n$, since the density fluctuation $\delta n = -\nabla\cdot(n\mathbf{u}_a)$ and the temperature fluctuation is given by $\delta T = (\partial T/\partial s)_n\nabla\cdot(sn_s\mathbf{u}_e/n)$. Roughly speaking, first sound is characterized by $\delta n \neq 0$ but $\delta T = 0$ and second sound by $\delta n = 0$ but $\delta T \neq 0$. Using the standard thermodynamic identities, after some straightforward but lengthy algebra, we arrive at $S = (1/2)\int d\mathbf{r}[\mathcal{S}^{(a)} + 2\mathcal{S}^{(ae)} + \mathcal{S}^{(e)}]$, where

$$\mathcal{S}^{(a)} = m\omega^2 n\mathbf{u}_a^2 - n\left(\frac{\partial P}{\partial n}\right)_{\bar{s}}(\nabla\cdot\mathbf{u}_a)^2 + \mathcal{S}^{(V)}, \quad (2)$$

$$\mathcal{S}^{(ae)} = \left(\frac{\partial P}{\partial s}\right)_n(\nabla\cdot\mathbf{u}_a)\left[\nabla\cdot\left(\frac{sn_s}{n}\mathbf{u}_e\right)\right], \quad (3)$$

$$\mathcal{S}^{(e)} = m\omega^2\frac{n_sn_n}{n}\mathbf{u}_e^2 - \left(\frac{\partial T}{\partial s}\right)_n\left[\nabla\cdot\left(\frac{sn_s}{n}\mathbf{u}_e\right)\right]^2, \quad (4)$$

and $\mathcal{S}^{(V)} \equiv (\nabla n\cdot\mathbf{u}_a)(\nabla V_T\cdot\mathbf{u}_a) + 2n(\nabla V_T\cdot\mathbf{u}_a)(\nabla\cdot\mathbf{u}_a)$ is the part directly related to the trapping potential V_T and $\bar{s} = s/n$ is the entropy per particle. It is clear that the first and second sound are governed by the actions $\mathcal{S}^{(a)}$ and $\mathcal{S}^{(e)}$, respectively. Their coupling is controlled by the term $\mathcal{S}^{(ae)}$, which generally is nonzero. In our case of a 2D Bose gas, the scale invariance leads to $(\partial P/\partial s)_n = T$, indicating that first and second sound are coupled at any nonzero temperature.

For a uniform superfluid ($V_T = 0$), the solutions of $\mathcal{S}^{(a)}$ and $\mathcal{S}^{(e)}$ are plane waves of wave vector q with dispersion $\omega_1 = c_1q$ and $\omega_2 = c_2q$, where $c_1 = \sqrt{(\partial P/\partial n)_{\bar{s}}/m}$, $c_2 = \sqrt{k_BT\bar{s}^2n_s/(m\bar{c}_vn_n)}$, and $\bar{c}_v$ is the specific heat per particle at constant volume. In Fig. 1, we report the temperature dependence of the decoupled first and second sound velocities at the coupling constant $g = 0.05$ by the black solid and red dashed lines, respectively, measured in unit of the zero temperature Bogoliubov sound velocity $c_B = \hbar\sqrt{gn}/m$. At the BKT transition temperature $T_c = 2\pi\hbar^2n/[mk_B\ln(\xi/g)]$, where $\xi = 380 \pm 3$

is a universal parameter [17, 18], the decoupled second sound velocity exhibits a discontinuity due to the universal jump in superfluid density. Including the coupling term $\mathcal{S}^{(ae)}$, we obtain the standard hydrodynamic equation for sound velocity u [2, 3]:

$$u^4 - u^2\left(c_1^2 + c_2^2\right) + c_1^2 c_2^2/\gamma = 0, \tag{5}$$

where $\gamma \equiv \bar{c}_p/\bar{c}_v$ is the ratio between specific heats at const pressure and volume. The coupling between first and second sound can be conveniently characterized by the so-called LP parameter $\epsilon_{\rm LP} = \gamma - 1$ [22, 25]. There are two solutions for the above hydrodynamic equation, u_1 and u_2, which in the absence of $\mathcal{S}^{(ae)}$ (i.e., $\gamma = 1$ or $\epsilon_{\rm LP} = 0$), coincide with the decoupled first and second sound velocities, c_1 and c_2. In Fig. 1, we present the velocities u_1 and u_2 by squares and circles, respectively. It is not a surprise to see that both velocities shows discontinuity at the BKT transition, as discussed in Ref. [12]. Remarkably, the sound velocities u_1 and u_2 differ largely from their decoupled counterparts c_1 and c_2, due to the large value of the LP parameter (see the inset). This is in sharp contrast to the cases of superfluid helium and unitary Fermi gas, where $\epsilon_{\rm LP} \sim 0$ and hence first and second sound couple very weakly. Nevertheless, near the transition, as shown by the dot-dashed line in Fig. 1, we find that the second sound velocity can still be approximated by $u_2 \simeq c_2/\sqrt{\gamma} = \sqrt{k_B T \bar{s}^2 n_s/(m\bar{c}_p n_n)}$ [25], indicating that the second sound could be well regarded a temperature wave at constant pressure.

The strong coupling between first and second sound is of great importance from the experimental point of view. In cold-atom experiments, temperature oscillations can not be directly measured. Thus, the characterization of second sound has to rely on the density measurement [16]. The strong coupling implies a large density fluctuation for second sound and thus makes its observation much easier. Indeed, at the constant pressure we find that the the ratio between the relative density and temperature fluctuations is given by,

$$\frac{\delta n/n}{\delta T/T} \simeq \frac{T}{n}\left(\frac{\partial n}{\partial T}\right)_P = -\epsilon_{\rm LP}, \tag{6}$$

as shown in the inset of Fig. 3(a). A large LP parameter therefore guarantees a significant density fluctuation of second sound for experimental observation.

We now consider the experimentally relevant harmonic traps. Focusing on an isotropic trapping potential ($\omega_x = \omega_y = \omega_\perp$) and compressional breathing modes (i.e., angular momentum $l = 0$), we may solve the variational action by inserting the following polynomial ansatz for the displacement fields [22]:

$$\mathbf{u}_a = \hat{\mathbf{r}}\sum_{i=0}^{N_p-1} A_i r^{i+1}, \mathbf{u}_e = \left[\frac{n\left(r\right)}{n_s\left(r\right)}\right]\hat{\mathbf{r}}\sum_{i=0}^{N_p-1} B_i r^{i+1}, \tag{7}$$

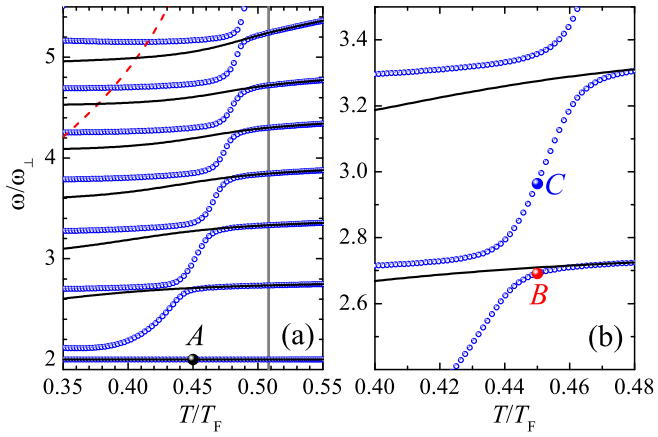

Figure 2: (Color online) (a) Breathing mode frequencies of a 2D Bose gas with $g = 0.05$ trapped in an isotropic harmoinc potential of frequency $\omega_\perp$. The full solutions calculated with $2N_p = 16$ variational parameters are shown by blue symbols, and the decoupled first and second sound solutions, ω_1 and ω_2, are plotted by solid and dashed lines, respectively. (b) A enlarged view of the left panel showing the hybridization between second sound and the $n = 1$ and $n = 2$ first sound modes. The density fluctuations at the points A, B and C are shown in Fig. 3(b). The temperature is measured in unit of a Fermi temperature $T_F = (2N)^{1/2}\hbar\omega_\perp/k_B$ of a 2D ideal spinless Fermi gas with the same number of atoms N as the Bose gas. The vertical gray line in (a) indicates the BKT transition temperature in traps. It should be note that the lowest $n = 0$ breathing mode with frequency $2\omega_\perp$ is an exact solution of Landau's two-fluid hydrodynamic equations [21].

where $\hat{\mathbf{r}}$ is the unit vector along the radial direction, $\{A_i, B_i\}$ $(i = 0, \cdots, N_p - 1)$ are the $2N_p$ variational parameters. The breathing mode frequencies are obtained by minimizing the action S with respect to these $2N_p$ parameters.

In Fig. 2(a), we show the discretized mode frequencies of the full two-fluid hydrodynamic action (blue symbols), as well as the decoupled first and second sound mode frequencies determined by $\mathcal{S}^{(a)}$ and $\mathcal{S}^{(e)}$ individually (black solid and red dashed lines, respectively). The decoupled sound mode frequencies differ largely from the full solutions, similar to the uniform case. Despite the large difference, we may still classify the first and second sound solutions as the horizontal and vertical branches, respectively. These solutions become degenerate at certain temperatures and hence exhibit clear avoided crossings with a typical distance $\Delta\omega \sim 0.2\omega_\perp$, as seen in the enlarged view of Fig. 2(b). We note that, for a unitary Fermi gas, similar avoided crossings have been predicted [22]. However, their structure (i.e., $\Delta\omega \sim 0.01\omega_\perp$) seems to be too small to observe experimentally.

It is evident that the second sound mode frequencies diverge towards the BKT transition. This peculiar behavior is caused by the universal jump in superfluid density. Approaching to the critical temperature T_c, the size R_s

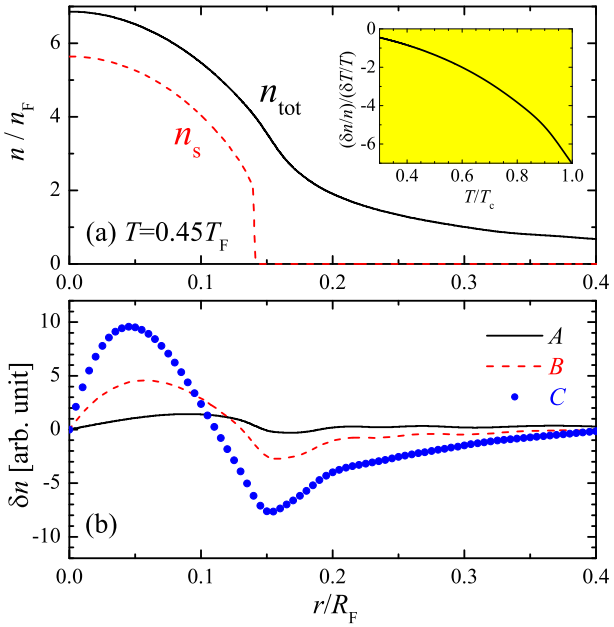

Figure 3: (Color online) (a) Density profile (solid line) and superfluid density profile (dashed line) of a trapped 2D Bose gas with $g = 0.05$ at $T = 0.45T_F$, in unit of the peak density n_F of a 2D ideal Fermi gas at $T = 0$. The inset shows the temperature dependence of the relative amplitude between density and temperature fluctuations of second sound in a uniform 2D Bose gas. (b) Density fluctuations (in arbitrary unit) of the lowest three two-fluid modes at the frequencies A, B and C, as indicated in Fig. 2.

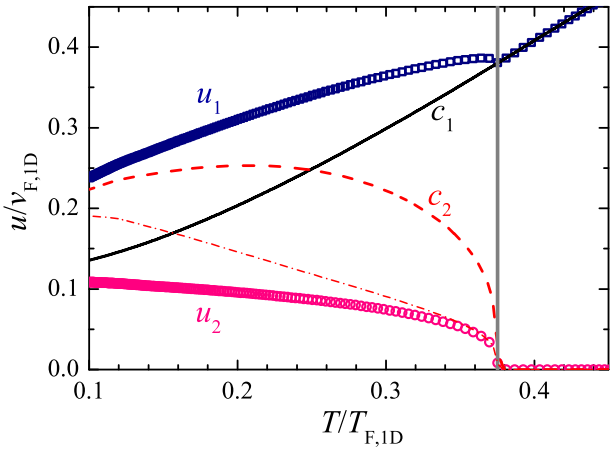

Figure 4: (Color online) Temperature dependence of the 1D first and second sound velocities (symbols), in unit of the Fermi velocity $v_F^{1D} = \sqrt{2k_BT_F^{1D}/m}$, where $k_BT_F^{1D} = (3\pi\hbar\omega_y/2)^{2/3}(\hbar^2n_1^2/2m)^{1/3}$ is the characteristic Fermi energy in quasi 1D and n_1 is the linear density. The solid and dashed lines show the decoupled first and second sound velocities, c_1 and c_2, respectively. The dot-dashed line is the second sound velocity with the leading-order correction in the sound coupling $c_2/\sqrt{\gamma}$.

of the superfluid component decreases as $R_s \propto \sqrt{T - T_c}$, leading to an increase in the minimum wave vector, $q \sim 1/R_s$. Using a finite second sound velocity c_2 at the transition, we find that $\omega_2 \sim c_2q \propto (T - T_c)^{-1/2}$ and therefore a divergent second sound mode frequency.

The strong coupling between first and second sound could lead to significant density fluctuations of second sound modes in harmonic traps, as shown in Fig. 3(b) for the lowest-two first sound (A, B) and the lowest second sound modes (C) near the BKT transition at $T = 0.45T_F \simeq 0.9T_c$. Surprisingly, the second sound mode gives much stronger density fluctuation than the first sound mode, implying that second sound is actually easier to excite and observe than the first sound. This finding, however, seems consistent with the earlier observation in the uniform case that, the relative amplitude between density and temperature fluctuations of second sounds - roughly given by the LP parameter - is very large near transition, as shown in the inset of Fig. 3(a).

We now turn to consider a highly anisotropic harmonic trap with $\omega_x \ll \omega_y$. We assume that the number of atoms is large enough so the system is still in the 2D regime where the local density approximation is applicable. However, its hydrodynamic behavior is strongly affected by the tight confinement in the y-axis. As discussed by Stringari and co-workers [26, 27], Landau's two-fluid hydrodynamic action S could reduce to a simplified 1D form, due to nonzero viscosity and thermal conductivity, which lead to invariant local fluctuations in temperature (δT) and chemical potential ($\delta\mu$) as a function of y for any low-energy modes with frequency $\omega \sim \omega_x \ll \omega_y$. In other words, we can integrate out the y coordinate in all the thermodynamic variables that enter the hydrodynamic action. More explicitly, we have a reduced Gibbs-Duhem relation, $\delta P_1 = s_1\delta T + n_1\delta\mu$, where the variables $P_1 = \int dyP(x, y)$, $s_1 = \int dys(x, y)$ and $n_1 = \int dyn(x, y)$ are the y-integrals of their 2D counterparts. All the 1D thermodynamic variables in the simplified 1D hydrodynamic action, except the superfluid density, can be derived from the reduced Gibbs-Duhem relation using the standard thermodynamic relations. Hydrodynamic modes in this quasi-1D configuration can then be solved using the same variational technique as in 2D.

In Fig. 4, we report the 1D first and second sound velocities for the case of a very weak trapping potential $\omega_x \sim 0$. This case is of particular interest since the propagation of sound waves can be directly observed through the density measurement. Indeed, both the sound velocities of first and second sound have been recently measured for a unitary Fermi gas in the similar quasi-1D configuration [16]. In contrast to the uniform 2D case, we find that the first and second sound velocities no longer exhibit a discontinuity across the BKT transition. However, there is an apparent kink in the first sound velocity at transition. This is because after the integral

over the y-coordinate, the 1D superfluid density $n_{s1} = \int dy n_s(x,y)$ now vanishes as $(T-T_c)^{1/2}$, approaching to the superfluid and normal fluid interface. As a result, the correction to the first sound velocity due to the sound coupling is given by $\Delta c_1 \simeq \epsilon_{\rm LP} c_2^2/[2(\epsilon_{\rm LP}+1)c_1] \sim (T-T_c)$ [25], which changes the slope of the velocity. We note that in the quasi-1D configuration, the coupling between first and second sound is again very strong, as indicated by $\epsilon_{\rm LP} \simeq 8$ at the BKT transition (not shown in Fig. 4).

The discretized mode frequency of first and second sound in the presence of a trapping frequency $\omega_x \neq 0$ can also be measured experimentally [15]. In this case, our calculations predict the similar pattern for mode frequencies as in Fig. 2. The second sound mode frequency diverges slower towards the BKT transition, $\omega_2 \propto (T-T_c)^{-1/4}$, due to the critical behavior $(T-T_c)^{1/2}$ of the reduced 1D superfluid density.

In conclusion, we have presented in this Letter various aspects of hydrodynamic modes of a 2D dilute Bose gas in harmonic traps. Differently from the superfluid helium and unitary Fermi gas, first and second sound have been found to strongly couple with each other. As a consequence, the second sound has a significant density fluctuation, whose relative amplitude is much larger than the temperature fluctuation. This makes the second sound much easier to excite and observe than in a unitary Fermi gas. We have predicted that the universal jump of superfluid density at the BKT transition leads to two peculiar features: (1) the breathing second sound mode frequency in an isotropic trap diverges like $(T-T_c)^{-1/2}$ and (2) the first sound velocity of a wave propagation in a highly anisotropic trap exhibit an apparent kink right at transition. The observation of these two features gives a strong evidence of the BKT physics. Our results apply as well to a 2D interacting Fermi gas, which has been recently realized in the cold-atom laboratory [28–30].

This research is supported by the ARC Discovery Projects (Grant Nos. FT130100815, DP140103231 and DP140100637) and NFRP-China (Grant No. 2011CB921502).

[1] L. Tisza, C. R. Phys. **207**, 1035 (1938).
[2] L. D. Landau, J. Phys. (USSR) **5**, 71 (1941).
[3] A. Griffin, T. Nikuni, and E. Zaremba, *Bose-Condensed Gases at Finite Temperatures* (Cambridge University Press, Cambridge, 2009).
[4] C.-L. Hung, X. Zhang, N. Gemelke, and C. Chin, Nature (London) **470**, 236 (2011).
[5] T. Yefsah, R. Desbuquois, L. Chomaz, K. J. Günter, and J. Dalibard, Phys. Rev. Lett. **107**, 130401 (2011).
[6] R. Desbuquois, L. Chomaz, T. Yefsah, J. Léonard, J. Beugnon, C. Weitenberg, and J. Dalibard, Nat. Phys. **8**, 645 (2012).
[7] L.-C. Ha, C.-L. Hung, X. Zhang, U. Eismann, S.-K. Tung, and C. Chin, Phys. Rev. Lett. **110**, 145302 (2013).
[8] P. C. Hohenberg, Phys. Rev. **158**, 383 (1967).
[9] N. D. Mermin and H. Wagner, Phys. Rev. Lett. **17**, 1133 (1966).
[10] V. L. Berezinskii, Sov. Phys. JETP **34**, 610 (1972).
[11] J. M. Kosterlitz and D. J. Thouless, J. Phys. C **5**, L124 (1972); J. Phys. C **6**, 1181 (1973).
[12] T. Ozawa and S. Stringari, Phys. Rev. Lett. **112**, 025302 (2014).
[13] A. Altmeyer, S. Riedl, C. Kohstall, M. J. Wright, R. Geursen, M. Bartenstein, C. Chin, J. Hecker Denschlag, and R. Grimm, Phys. Rev. Lett. **98** 040401 (2007).
[14] J. Joseph, B. Clancy, L. Luo, J. Kinast, A. Turlapov, and J. E. Thomas, Phys. Rev. Lett. **98**, 170401 (2007).
[15] M. K. Tey, L. A. Sidorenkov, E. R. Sánchez Guajardo, R. Grimm, M. J. H. Ku, M. W. Zwierlein, Y. H. Hou, L. Pitaevskii, and S. Stringari, Phys. Rev. Lett. **110**, 055303 (2013).
[16] L. A. Sidorenkov, M. K. Tey, R. Grimm, Y.-H. Hou, L. Pitaevskii, and S. Stringari, Nature (London) **498**, 78 (2013).
[17] N. Prokof'ev, O. Ruebenacker, and B. Svistunov, Phys. Rev. Lett. **87**, 270402 (2001).
[18] N. Prokof'ev and B. Svistunov, Phys. Rev. A **66**, 043608 (2002).
[19] A. Rançon and N. Dupuis, Phys. Rev. A **85**, 063607 (2012).
[20] E. Taylor and A. Griffin, Phys. Rev. A **72**, 053630 (2005).
[21] E. Taylor, H. Hu, X.-J. Liu, and A. Griffin, Phys. Rev. A **77**, 033608 (2008).
[22] E. Taylor, H. Hu, X.-J. Liu, L. P. Pitaevskii, A. Griffin, and S. Stringari, Phys. Rev. A **80**, 053601 (2009).
[23] P. R. Zilsel, Phys. Rev. **79**, 309 (1950).
[24] L. P. Pitaevskii and A. Rosch, Phys. Rev. A **55**, R853 (1997).
[25] H. Hu, E. Taylor, X.-J. Liu, S. Stringari, and A. Griffin, New J. Phys. **12**, 043040 (2010).
[26] G. Bertaina, L. P. Pitaevskii, and S. Stringari, Phys. Rev. Lett. **105**, 150402 (2010).
[27] Y.-H. Hou, L. P. Pitaevskii, and S. Stringari, Phys. Rev. A **88**, 043630 (2013).
[28] K. Martiyanov, V. Makhalov, and A. Turlapov, Phys. Rev. Lett. **105**, 030404 (2010).
[29] B. Fröhlich, M. Feld, E. Vogt,M. Koschorreck,W. Zwerger, and M. Köhl, Phys. Rev. Lett. **106**, 105301 (2011).
[30] A. A. Orel, P. Dyke, M. Delehaye, C. J. Vale, and H. Hu, New J. Phys. **13**, 113032 (2011).